ISSN 1070-3284, Russian Journal of Coordination Chemistry, 2022, Vol. 48, No. 1, pp. 60–68. © Pleiades Publishing, Ltd., 2022.

Syntheses, Structures, Luminescence Properties of Two Coordination Polymers Constructed by a Semirigid Aromatic Multicarboxylite Ligand

Y. C. Sun[a, *], Q. Q. Wei[a], Q. X. Wang[a], and J. S. Zhao[b]

[a] *College of Chemistry and Environmental Engineering, Sichuan University of Science and Engineering, Zigong, 643000 P.R. China*

[b] *Key Laboratory of Synthetic and Natural Functional Molecule Chemistry of Ministry of Education, Shaanxi Key Laboratory of Physical-Inorganic Chemistry, Xi'an, 710069 P.R. China*

**e-mail: sunyanchun2000@sina.com*

Received January 12, 2021; revised July 6, 2021; accepted July 8, 2021

Abstract—Two new coordination polymers, namely $\{[Zn_3(bcpmba)_2(Py)_6]\cdot 2H_2O\}_n$ (**I**) and $\{[Cd(Hbcpmba)]\cdot H_2O\}_n$ (**II**) (H_3bcpmba = 3,5-bi(4-carboxy-phenylene-methylene-oxy)-benzoic acid, Py = pyridine) have been synthesized under hydrothermal conditions. All the compounds are characterized using powder X-ray diffraction (CIF file. CCDC nos. 2051308 (**I**) and 2051312 (**II**)), IR spectra, thermal stability analysis, and elemental analyses. Compounds **I** and **II** are all 2D porous CPs. The effects of the $bcpmba^{3-}$ anions, and the N-donor ligands on the structures of the coordination polymers have been discussed. Moreover, their photoluminescence properties and thermal stability of them have been investigated.

Keywords: coordination polymers, 3,5-bi(4-carboxy-phenylene-methylene-oxy)-benzoic acid, crystal structures, photoluminescence

DOI: 10.1134/S1070328422010067

INTRODUCTION

Coordination polymers (CPs) have attracted extensive attention in supramolecular chemistry and crystal engineering due to their fascinating structures and various potential applications, such as in adsorption, separation, sensors, and catalysis [1–3]. Great progress has been made in the preparation of polymers in recent years. A large number of complexes with novel structures and excellent properties have been synthesized [4, 5]. However, precise control of the coordination polymers structure from a self-assembly system is still exceedingly difficult because subtle factors may affect the assembly process. The nature of the ligand, metal ion, the metal–ligand ratio, temperature, and other factors can influence the final topology of the CPs, leading to unexpected structural diversity [6]. Among these, the type of organic ligand represents a particularly interesting variable to modify, allowing the generation of potentially desired products [7]. In this regard, polycarboxylic acids containing several aromatic rings with variable positions of the –COOH functionalities represent one of the most compelling classes of organic ligands, especially when dealing with the synthesis of new coordination polymers (CPs) [8]. This is primarily governed by their ability to adopt a large diversity of coordination modes depending on the degree of deprotonation in the course of hydrothermal reactions [9]. The semi-rigid ligand can timely fine tune its conformation to adapt the coordination geometry of metal centers, leading to the structural diversities of targeted products [10].

As an extension of our research on the hydrothermal synthesis of new first-row transition metal CPs and complexes driven by polycarboxylate blocks, herein we have centered our attention on a symmetrical V-shaped semirigid aromatic multicarboxylite ligand (H_3bcpmba, Scheme 1) to construct coordination polymers.

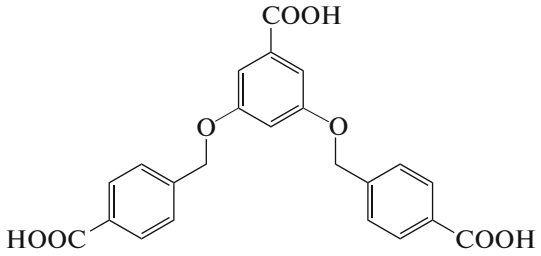

Scheme 1.

H_3bcpmba is chosen to fabricate porous CPs based on the following advantages: (i) H_3bcpmba with three carboxylic groups possesses multiple coordination sites and various coordination modes, which is bene-

ficial to produce fascinating frameworks [11]; (ii) the three benzene rings in H_3bcpmba can brace the space, which is beneficial for the formation of porous CPs. (iii) the –O– and $-CH_2-$ motif can increase the flexibility of ligands, which can better meet the coordination requirements of metal ions [12]. It is well known that the use of mix-ligand is a good choice for the construction of new polymeric structures [13]. Multidentate N-donor ligands, such as 4,4'-bipyridine, 2,2'-bipyridine, and pyridine have been employed as auxiliary ligands in the fabrication of CPs. Thus, in this study, pyridine as neutral ligands have been successfully used as auxiliary ligand. Also, CPs based on d^{10} metal centers and conjugated organic linkers attract continuous interest from chemists due to their various applications in photochemistry, chemical sensors, and light-emitting diodes [14].

Based on these considerations, we report the preparation of two new CPs with the H_3bcpmba ligand and Py, $\{[Zn_3((bcpmba)^{3-})_2(Py)_6]\cdot 2H_2O\}_n$ (**I**) and $\{[Cd((Hbcpmba)^{2-})]\cdot H_2O\}_n$ (**II**). Their single crystal structures, thermal stability, and luminescent properties are systematically investigated.

EXPERIMENTAL

Materials and general methods. All reagents were from commercial sources (analytical reagent grade) and were used as received. H_3bcpmba ligand was purchased from Jinan Henghua Sci. & Tec. Co. Ltd. Infrared spectra were measured on a Nicolet Avatar 360 FTIR instrument from 4000 to 400 cm^{-1} using KBr pellets. Elemental analyses of C, H, and N were carried out on a Perkin-Elmer 2400 CHNS Elemental Analyzer. Powder X-ray diffraction (PXRD) was performed on a Bruker D8 ADVANCE X-ray powder diffractometer with CuK_α radiation (λ = 1.5406 Å). Thermogravimetric (TG) analyses were performed on a Netzsch TG209F3 thermogravimetric analyzer from 30 to 900°C at 5°C min^{-1} under N_2. The luminescence spectra were performed on an Aminco Bowman Series 2 Luminescence spectrometer at room temperature.

Synthesis of $\{[Zn_3(bcpmba)_2(Py)_6]\cdot 2H_2O\}_n$ (I). A mixture of $ZnSO_4\cdot 7H_2O$ (29 mg, 0.1 mmol) and H_3bcpmba (21 mg, 0.05 mmol) was added to a mixed solvent system containing acetonitrile (4 mL) and water (2 mL) which was stirred about 10 min in air, then drop Py (98 mg, 1.2 mmol) in mixed system. The contents were first sealed in a 25 mL Teflon-lined stainless vessel and heated at 160°C for 72 h and then gradually cooled to room temperature at a rate of 5°C h^{-1}. Colorless rod-like crystals of **I** were collected by filtration and washed with methanol and ethanol. The yield was 13 mg (25% based on Zn). Calcd. (Found) for $C_{76}H_{64}N_6O_{18}Zn_3$: C, 59.01 (59.03); H, 4.14 (4.12); N, 5.44 (5.40)%.

IR (KBr pellet; ν, cm^{-1}): 3776 w, 3435 s, 3059 m, 2918(m), 1954 w, 1608 s, 1363 s, 1153 s, 1043 s, 775 s, 673 m, 573 w.

Synthesis of $\{[Cd(Hbcpmba)]\cdot H_2O\}_n$ (II). The procedure was similar to the preparation of **I**, except that $ZnSO_4\cdot 7H_2O$ was replaced with $Cd(NO_3)_2\cdot 4H_2O$ and do not drop Py. The yield was 25 mg (45% based on Cd). Calcd. (Found) for $C_{23}H_{17}O_8Cd$: C, 51.71 (51.68); H, 3.18 (3.15); N, 0.00 (0.00)%.

IR (KBr pellet; ν, cm^{-1}): 3438 w, 3039 w, 2875 w, 1552 s, 1367 s, 1159 s, 1059 m, 828 m, 773 m, 528 w.

X-ray crystallography. Crystallographic data for the compounds were collected on a Bruker Apex Smart CCD diffractometer with graphite-monochromated MoK_α radiation (λ = 0.71073 Å) using the ω-scan technique at room temperature. SAINT software was used for data integration and reduction [15]. Absorption correction was performed with SADABS [16]. All the structures were solved by the direct method employing SHELXS-97 and SHELXL-97 was used to refine on F^2 with the full-matrix least-squares technique [17, 18]. The non-hydrogen atoms were refined with the anisotropic displacement parameters. The hydrogen atoms were set in calculated positions and refined as riding atoms with a common isotropic thermal parameter. The contribution of the electron density by the remaining disorder solvent molecule in the channels of **I** and **II** were removed by the SQUEEZE routine in PLATON [19]. Details of the crystal parameters, data collections, and refinement for **I**, **II** are summarized in Table 1, elected bond length and bond angles are listed in Table 2.

Crystallographic data (excluding structure factors) for the structures in this paper were deposited in the Cambridge Crystallographic Data Centre (CCDC nos. 2051308 (**I**) and 2051312 (**II**); deposit@ccdc.cam.ac.uk, http://www.ccdc.cam. ac.uk).

RESULTS AND DISCUSSION

The IR spectra of compounds **I** and **II** are similar (Figs. S1, S2). In the IR spectra of **I** and **II**, the bands at 3435 cm^{-1} for **I** and 3438 cm^{-1} for **II** are assigned to O–H stretching vibration, which indicate the presence of water molecules in **I** and **II**. The bands of asymmetric stretching vibration of carboxylate groups appear at 1608 and 1552 cm^{-1}, the symmetric stretching vibrations appear at 1363 and 1367 cm^{-1}, respectively. The splitting of ν_{as}(COO) and ν_s(COO) suggests that the carboxylate groups of ligand take different coordination modes. In addition, the spectra of **I** and **II** show bands at 3059 and 3039 cm^{-1}, which are attributed to the stretching vibration of aromatic C–H bonds. All these facts are well consistent with the single crystal X-ray diffraction results.

Compound **I** crystallizes in a monoclinic crystal system with the space group of *C2/c*. As shown in

Table 1. Crystallographic data and refinement details for structures **I** and **II***

Compound	**I**	**II**
Empirical formula	$C_{76}H_{64}N_6O_{18}Zn_3$	$C_{23}H_{17}O_8Cd$
Formula weight	1545.44	533.77
T, K	296.15	293(2)
Crystal system	Monoclinic	Orthorhombic
Space group	$C2/c$	$Pnma$
a, Å	12.645(2)	18.8844(15)
b, Å	21.776(4)	4.7177(4)
c, Å	26.802(6)	24.6317(19)
α, deg	90	90
β, deg	101.922(4)	90
γ, deg	90	90
V, Å^3	7221(2)	2194.5(3)
Z	4	4
ρ_{calc}, mg mm^{-3}	1.422	1.616
μ, mm^{-1}	1.063	1.042
F(000)	3184.0	1068.0
Crystal size, mm^3	0.11 × 0.1 × 0.09	0.18 × 0.12 × 0.08
2θ range for data collection, deg	3.106 to 50.02	2.718 to 50.014
Index ranges	$-15 \le h \le 14$, $-19 \le k \le 25$, $-31 \le l \le 31$	$-22 \le h \le 22$, $-5 \le k \le 5$, $-21 \le l \le 29$
Reflections collected	17955	10754
Independent reflections	6347	2200
R_{int}	0.0950	0.0534
Data/restraints/parameters	6347/0/468	2200/162/236
Goodness-of-fit on F^2	0.966	1.191
Final R indexes ($I > 2\sigma(I)$)	$R_1 = 0.0650$, $wR_2 = 0.1421$	$R_1 = 0.0883$, $wR_2 = 0.2830$
Final R indexes (all data)	$R_1 = 0.1560$, $wR_2 = 0.1849$	$R_1 = 0.0960$, $wR_2 = 0.2925$
Largest diff. peak/hole, e Å^{-3}	0.46/−0.39	1.35/−1.60

* $R_1 = \sum \| F_o | - | F_c \| / \sum | F_o |$, $wR_2 = \left[\sum w \left(F_o^2 - F_c^2 \right)^2 \Big/ \sum w \left(F_o^2 \right)^2 \right]^{1/2}$.

Fig. 1, the structure of **I** contains three crystallographically independent Zn(II) ions, two completely deprotonated (bcpmba)$^{3-}$ ligand, six Py ligands, and two lattice water molecules. The Zn(1) ion is coordinated by four O atoms (O(7), O(8), O(5)$^{\#1}$, O(6)$^{\#1}$) from two individual bcpmba^{3-} anions, and two N atoms (N(1), N(2)) from two Py ligands, resulting in a greatly distorted octahedral geometry. The equatorial plane is occupied by O(5)$^{\#1}$, O(7), N(1), N(2), while O(6)$^{\#1}$, O(8) fill the axial positions. The Zn(2) ion also shows a six-coordinated greatly distorted octahedral geometry, with four coordinated O atoms come from two individual (bcpmba)$^{3-}$ ligands (O(1), O(2), O(1)$^{\#2}$, O(2)$^{\#2}$) in the equatorial plane and two coordinated N atoms from two Py ligands (N(3), N(2)$^{\#2}$) occupying the apical positions. Through the bridging of (bcpmba)$^{3-}$ anions the coordination mode of bidentate chelating was adopted; metal ions are connected to generate a 2D porous lay structure (Fig. 2). The Zn–O bonds range from 2.232(3) to 2.410(3) Å and the Zn–N distances are from 2.309(4) to 2.347(4) Å, comparable to similar complexes reported in [20]. Lattice H_2O molecules are embedded into the surface of the pores. About 3.9% potential solvent-accessible volume is estimated by using PLATON software. The volume does not contain the guest molecules (H_2O).

Compound **II** crystallizes in monoclinic space group $P2_1/n$. As shown in Fig. 3, the independent unit of **II** is composed of one Cd(1) ion, one partly deprotonated (Hbcpmba)$^{2-}$ ligands, and one lattice water molecule. The Cd(1) ion is coordinated by six O atoms and shows slightly distorted octahedral geometries.

Table 2. Selected bond length (Å) and bond angles (deg) for compound **I** and **II***

Bond	*d*, Å	Bond	*d*, Å
		I	
Zn(1)–O(6)$^{\#1}$	1.972(4)	Zn(2)–O(1)$^{\#2}$	1.987(4)
Zn(1)–O(7)	2.039(5)	Zn(2)–O(1)	1.987(4)
Zn(1)–O(8)	2.382(6)	Zn(2)–N(3)	2.048(6)
Zn(1)–N(1)	2.043(6)	Zn(2)–N(3)$^{\#2}$	2.048(6)
Zn(1)–N(2)	2.067(5)	O(6)–Zn(1)$^{\#3}$	1.972(4)
Zn(1)–C(15)	2.531(8)		
		II	
Cd(1)–O(1)$^{\#1}$	2.354(17)	Cd(1)–O(8)	2.249(16)
Cd(1)–O(1)$^{\#2}$	2.354(17)	Cd(1)–O(8)$^{\#10}$	2.249(16)
Cd(1)–O(4)$^{\#3}$	2.283(18)	Cd(1)–O(8)$^{\#11}$	2.381(17)
Cd(1)–O(4)$^{\#4}$	2.283(18)	O(1)–Cd(1)$^{\#12}$	2.354(16)
Cd(1)–O(5)$^{\#5}$	2.299(17)	O(4)–Cd(1)$^{\#15}$	2.283(18)
Cd(1)–O(5)$^{\#6}$	2.299(17)	O(5)–Cd(1)$^{\#17}$	2.299(17)
Cd(1)–O(7)$^{\#7}$	2.187(17)	O(7)–Cd(1)$^{\#7}$	2.188(17)
Cd(1)–O(7)$^{\#8}$	2.187(17)	O(8)–Cd(1)$^{\#11}$	2.381(17)
Cd(1)–O(8)$^{\#9}$	2.381(17)		
Angle	ω, deg	Angle	ω, deg
		I	
O(6)$^{\#1}$Zn(1)O(7)	103.7(2)	C(23)O(6)Zn(1)$^{\#3}$	110.4(4)
O(6)$^{\#1}$Zn(1)O(8)	161.6(2)	C(15)O(7)Zn(1)	98.3(5)
O(6)$^{\#1}$Zn(1N(1)	106.5(2)	C(15)O(8)Zn(1)	82.0(5)
O(6)$^{\#1}$Zn(1)N(2)	93.6(2)	C(24)N(1)Zn(1)	124.0(6)
O(6)$^{\#1}$Zn(1)C(15)	132.5(3)	C(28)N(1)Zn(1)	122.3(6)
O(7)Zn(1)O(8)	58.14(19)	C(34)N(2)Zn(1)	121.3(5)
O(7)Zn(1)N(1)	135.6(2)	C(29)N(3)Zn(2)	125.6(7)
O(7)Zn(1)N(2)	104.5(2)	C(33)N(3)Zn(2)	118.0(6)
O(7)Zn(1)C(15)	28.8(2)	O(7)C(15)Zn(1)	52.8(4)
O(8)Zn(1)C(15)	29.3(2)	O(8)C(15)Zn(1)	68.7(4)
N(1)Zn(1)O(8)	87.3(2)	C(11)C(15)Zn(1)	173.6(6)
N(1)Zn(1)N(2)	105.2(2)	O(1)Zn(2)N(3)	109.1(2)
N(1)Zn(1)C(15)	112.4(3)	O(1)Zn(2)N(3)$^{\#2}$	99.8(2)
N(2)Zn(1)O(8)	94.3(2)	O(1)$^{\#2}$Zn(2)N(3)	99.8(2)
N(2)Zn(1)O(15)	101.2(2)	O(1)$^{\#2}$Zn(2)N(3)$^{\#2}$	109.1(2)
O(1)Zn(2)O(1)$^{\#2}$	101.0(3)	N(3)Zn(2)N(3)$^{\#2}$	133.9(4)
C(1)O(1)Zn(2)	105.8(5)		
		II	
O(1)$^{\#1}$Cd(1)O(1)$^{\#2}$	42.3(10)	O(7)$^{\#9}$Cd(1)O(7)$^{\#10}$	66.9(11)
O(1)$^{\#2}$Cd(1)O(8)$^{\#3}$	115.3(6)	O(7)$^{\#10}$Cd(1)O(8)$^{\#11}$	123.5(7)
O(1)$^{\#1}$Cd(1)O(8)$^{\#3}$	84.9(6)	O(7)$^{\#10}$Cd(1)O(8)$^{\#4}$	34.3(6)
O(1)$^{\#1}$Cd(1)O(8)$^{\#4}$	115.3(6)	O(7)$^{\#9}$Cd(1)O(8)$^{\#4}$	87.8(6)

Table 2. (Contd.)

Angle	ω, deg	Angle	ω, deg
O(4)$^{\#5}$Cd(1)O(1)$^{\#2}$	85.8(6)	O(7)$^{\#10}$Cd(1)O(8)$^{\#3}$	87.8(6)
O(4)$^{\#6}$Cd(1)O(1)$^{\#1}$	85.8(6)	O(7)$^{\#9}$Cd(1)O(8)	123.5(7)
O(4)$^{\#5}$Cd(1)O(1)$^{\#1}$	114.9(6)	O(7)$^{\#10}$Cd(1)O(8)	103.2(7)
O(4)$^{\#6}$Cd(1)O(1)$^{\#2}$	114.9(6)	O(7)$^{\#9}$Cd(1)O(8)$^{\#3}$	34.3(6)
O(4)$^{\#5}$Cd(1)O(4)$^{\#6}$	86.3(9)	O(8)$^{\#11}$Cd(1)O(1)$^{\#2}$	175.5(7)
O(4)$^{\#5}$Cd(1)O(5)$^{\#7}$	86.4(6)	O(8)Cd(1)O(1)$^{\#1}$	175.5(7)
O(4)$^{\#5}$Cd(1)O(5)$^{\#8}$	31.7(6)	O(8)Cd(1)O(1)$^{\#2}$	141.8(7)
O(4)$^{\#6}$Cd(1)O(5)$^{\#7}$	31.7(6)	O(8)$^{\#11}$Cd(1)O(1)$^{\#1}$	141.8(7)
O(4)$^{\#6}$Cd(1)O(5)$^{\#8}$	86.4(6)	O(8)Cd(1)O(4)$^{\#6}$	90.0(6)
O(4)$^{\#6}$Cd(1)O(8)$^{\#4}$	158.7(5)	O(8)Cd(1)O(4)$^{\#5}$	66.3(6)
O(4)$^{\#5}$Cd(1)O(8)$^{\#4}$	87.4(6)	O(8)$^{\#11}$Cd(1)O(4)$^{\#5}$	90.0(6)
O(4)$^{\#6}$Cd(1)O(8)$^{\#3}$	87.4(6)	O(8)$^{\#11}$Cd(1)O(4)$^{\#6}$	66.3(6)
O(4)$^{\#5}$Cd(1)O(8)$^{\#3}$	158.7(5)	O(8)Cd(1)O(5)$^{\#8}$	98.1(6)
O(5)$^{\#7}$Cd(1)O(1)$^{\#2}$	83.3(6)	O(8)$^{\#11}$Cd(1)O(5)$^{\#7}$	98.1(6)
O(5)$^{\#8}$Cd(1)O(1)$^{\#1}$	83.3(6)	O(8)Cd(1)O(5)$^{\#7}$	118.5(6)
O(5)$^{\#7}$Cd(1)O(1)$^{\#1}$	57.8(6)	O(8)$^{\#11}$Cd(1)O(5)$^{\#8}$	118.5(6)
O(5)$^{\#8}$Cd(1)O(1)$^{\#2}$	57.8(6)	O(8)Cd(1)O(8)$^{\#4}$	68.9(6)
O(5)$^{\#8}$Cd(1)O(5)$^{\#7}$	70.4(9)	O(8)$^{\#11}$Cd(1)O(8)	34.1(10)
O(5)$^{\#8}$Cd(1)O(8)$^{\#4}$	98.7(6)	O(8)$^{\#11}$Cd(1)O(8)$^{\#3}$	68.9(6)
O(5)$^{\#8}$Cd(1)O(8)$^{\#3}$	167.1(6)	O(8)Cd(1)O(8)$^{\#3}$	93.3(4)
O(5)$^{\#7}$Cd(1)O(8)$^{\#4}$	167.1(6)	O(8)$^{\#11}$Cd(1)O(8)$^{\#4}$	93.3(4)
O(5)$^{\#7}$Cd(1)O(8)$^{\#3}$	98.7(6)	O(8)$^{\#3}$Cd(1)O(8)$^{\#4}$	91.1(9)
O(7)$^{\#9}$Cd(1)O(1)$^{\#1}$	56.2(6)	O(1)$^{\#12}$O(1)Cd(1)$^{\#13}$	68.8(5)
O(7)$^{\#10}$Cd(1)O(1)$^{\#2}$	56.2(6)	C(1)O(1)Cd(1)$^{\#13}$	129.5(15)
O(7)$^{\#10}$Cd(1)O(1)$^{\#1}$	80.9(7)	O(4)$^{\#15}$O(4)Cd(1)$^{\#16}$	133.1(5)
O(7)$^{\#9}$Cd(1)O(1)$^{\#2}$	80.9(7)	O(5)$^{\#15}$O(4)Cd(1)$^{\#16}$	74.8(11)
O(7)$^{\#9}$Cd(1)O(4)$^{\#5}$	166.3(7)	C15O(4)Cd(1)$^{\#16}$	131.0(13)
O(7)$^{\#10}$Cd(1)O(4)$^{\#6}$	166.3(7)	O(4)$^{\#15}$O(5)Cd(1)$^{\#17}$	73.5(11)
O(7)$^{\#9}$Cd(1)O(4)$^{\#6}$	102.5(7)	C(15)O(5)Cd(1)$^{\#17}$	131.5(14)
O(7)$^{\#10}$Cd(1)O(4)$^{\#5}$	102.5(7)	O(8)$^{\#11}$O(7)Cd(1)$^{\#9}$	80.6(10)
O(7)$^{\#10}$Cd(1)O(5)$^{\#7}$	137.1(7)	C(23)O(7)Cd(1)$^{\#9}$	131.1(14)
O(7)$^{\#9}$Cd(1)O(5)$^{\#7}$	95.5(7)	Cd(1)O(8)Cd(1)$^{\#4}$	111.1(6)
O(7)$^{\#9}$Cd(1)O(5)$^{\#8}$	137.1(7)	O(7)$^{\#11}$O(8)Cd(1)$^{\#4}$	65.0(10)
O(7)$^{\#10}$Cd(1)O(5)$^{\#8}$	95.5(7)	O(7)$^{\#11}$O(8)Cd(1)	175.6(15)
O(8)$^{\#11}$O(8)Cd(1)	73.0(5)	O(8)$^{\#11}$O(8)Cd(1)$^{\#4}$	135.6(4)
C(23)O(8)Cd(1)	124.0(13)	C(23)O(8)Cd(1)$^{\#4}$	121.8(12)

* Symmetry codes: $^{\#1}$ $5/2-x, 1/2+y, 1/2-z$; $^{\#2}$ $1-x, +y, -1/2-z$; $^{\#3}$ $5/2-x, -1/2+y, 1/2-z$ for **I**. $^{\#1}$ $1+x, 2+y, +z$; $^{\#2}$ $1+x, 1/2-y, +z$; $^{\#3}$ $2-x, 1/2+y, 1-z$; $^{\#4}$ $2-x, 2-y, 1-z$; $^{\#5}$ $1/2+x, 3/2-y, 1/2-z$; $^{\#6}$ $1/2+x, 1+y, 1/2-z$; $^{\#7}$ $1/2+x, 5/2-y, 1/2-z$; $^{\#8}$ $1/2+x, +y, 1/2-z$; $^{\#9}$ $2-x, 3-y, 1-z$; $^{\#10}$ $2-x, -1/2+y, 1-z$; $^{\#11}$ $+x, 5/2-y, +z$; $^{\#12}$ $+x, -3/2-y, +z$; $^{\#13}$ $-1+x, -2+y, +z$; $^{\#14}$ $+x, 1/2-y, +z$; $^{\#15}$ $+x, 3/2-y, +z$; $^{\#16}$ $-1/2+x, -1+y, 1/2-z$; $^{\#17}$ $-1/2+x, +y, 1/2-z$; $^{\#18}$ $+x, -1/2-y, +z$ for **II**.

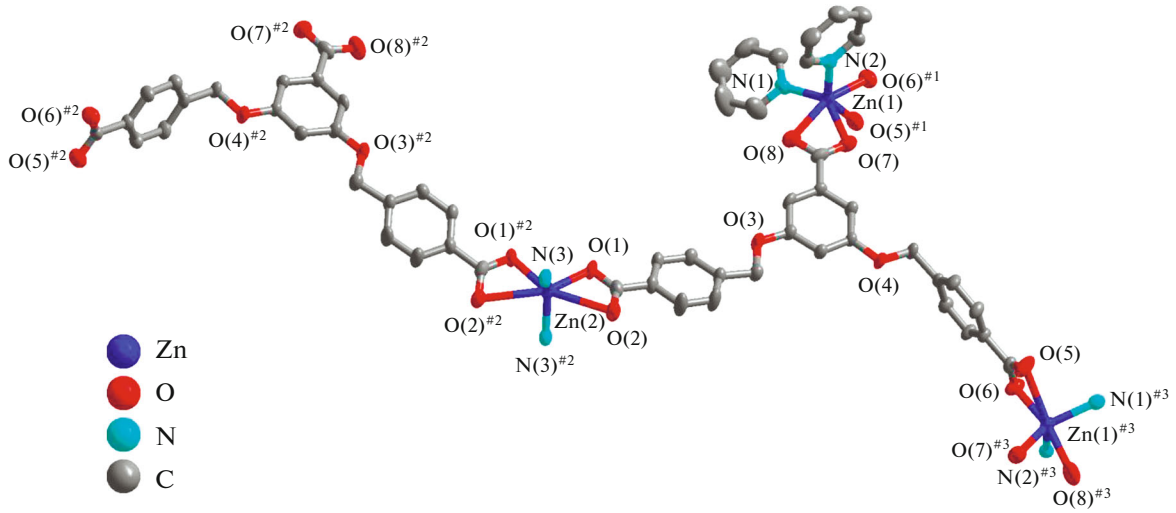

Fig. 1. Crystal structure of **I**: coordination environment of Zn(II) in **I** showing 30% probability displacement ellipsoids (H atoms are omitted for clarity). Symmetry code: #1 $5/2 - x, 1/2 + y, 1/2 - z$; #2 $1 - x, y, -1/2 - z$; #3 $5/2 - x, -1/2 + y, 1/2 - z$.

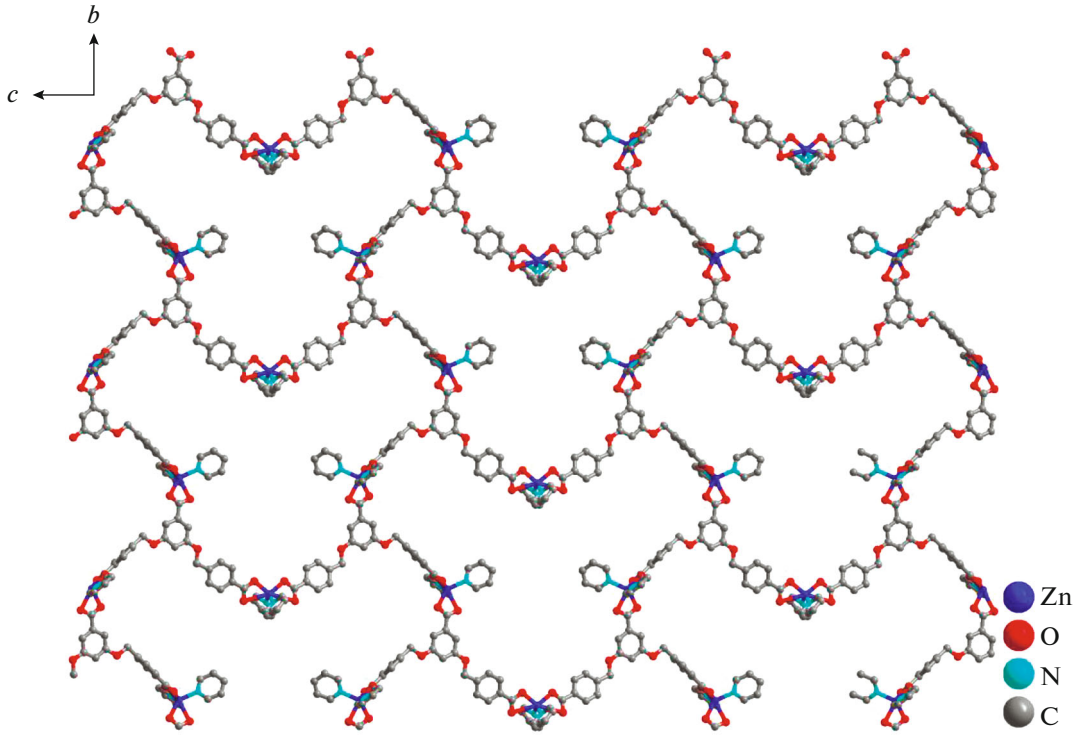

Fig. 2. The 2D pore layer in the *bc* plane of coordination polymer **I**.

The six O atoms around Cd(II) ion come from four individual $Hbcpmba^{2-}$ anions. The Cd(II) ion is situated at the center of the octahedron. O(1), $O(2)^{\#3}$, $O(7)^{\#1}$, and $O(8)^{\#5}$ locate the equatorial plane. $O(5)^{\#4}$ and $O(8)^{\#4}$ occupy the two axial positions (Fig. 3). The Cd–O bonds range from 2.177(1) to 2.357(1) Å. The Cd atoms form binuclear units by common oxygen atoms, and the binuclear units further form a 2D porous structure by bridging carboxyl groups adopt monodentate, bidentate chelating, and tridentate chelating coordination modes (Fig. 4). Lattice H_2O molecules are embedded into the surface of the pores. About 17.1% potential solvent-accessible volume is

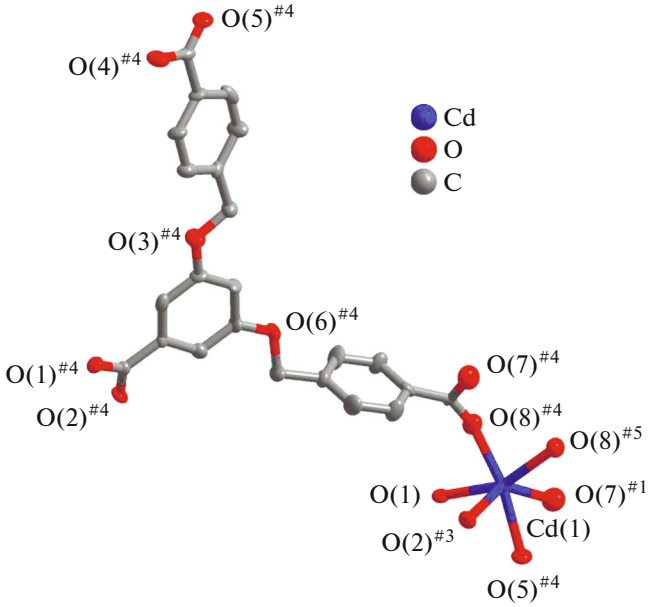

Fig. 3. Crystal structure of **II**: Coordination environment of Cd(II) in **II** showing 30% probability displacement ellipsoids (H atoms are omitted for clarity). Symmetry code: #1 1 + *x*, 2 + *y*, +*z*; #2 +*x*, 1/2 – *y*, +*z*; #3 2 – *x*, 1/2 + *y*, 1 – *z*; #4 2 – *x*, 2 – *y*, 1 – *z*; #5 1/2 + *x*, 3/2 – *y*, 1/2 – *z*; #6 1/2 + *x*, 1 + *y*, 1/2 – *z*; #7 1/2 + *x*, 5/2 – *y*, 1/2 – *z*; #8 1/2 + *x*, +*y*, 1/2 – *z*; #9 2 – *x*, 3 – *y*, 1 – *z*; #10 2 – *x*, –1/2 + *y*, 1 – *z*; #11 +*x*, 5/2 – *y*, +*z*; #12 *x*, –3/2 – *y*, +*z*; #13 –1 + *x*, –2 + *y*, +*z*; #14 +*x*, 1/2 – *y*, +*z*; #15 +*x*, 3/2 – *y*, +*z*; #16 –1/2 + *x*, –1 + *y*, 1/2 – *z*; #17 –1/2 + *x*, +*y*, 1/2 – *z*; #18 +*x*, –1/2 – *y*, +*z*.

estimated by using PLATON software. The volume does not contain the guest molecules (H_2O).

Based on the above descriptions, we found that the H_3bcpmba ligand adopting the same "Y" conformation but the different coordination modes, so we concluded that coordination modes play crucial roles in determining the final structure of the targeted product [22, 23]. In coordination polymer **I**, the three carboxylic groups of the ligand adopt bidentate chelating coordination mode (Fig. 5a). In coordination polymer **II**, the ligand adopt monodentate, bidentate chelating, and tridentate chelating coordination modes (Fig. 5b). Besides, the auxiliary ligand can influence the final structure of complexes. Comparing the structures of the two complexes, it was found that the main reason for the structural differences was that the presence of N-donor ligand and metal polyhedron geometry. In complex **I**, N-donor blocks coordination places of Zn effectively blocked the coordination of zinc ions. According to the above-mentioned analysis, we conclude that the coordination mode of the main ligand plays a decisive role in the structure of the complex, while the auxiliary ligand has a certain influence on the structure of the complex.

To evaluate the thermal stability of compounds **I** and **II**, they were subjected to TG analysis that was carried out under a nitrogen atmosphere from 30 to 900°C (Fig. 6). Compound **I** loses its two coordinated water molecules (obsd., 2.54%; calcd., 2.32%) in the 30–77°C temperature range. Then, **I** released six

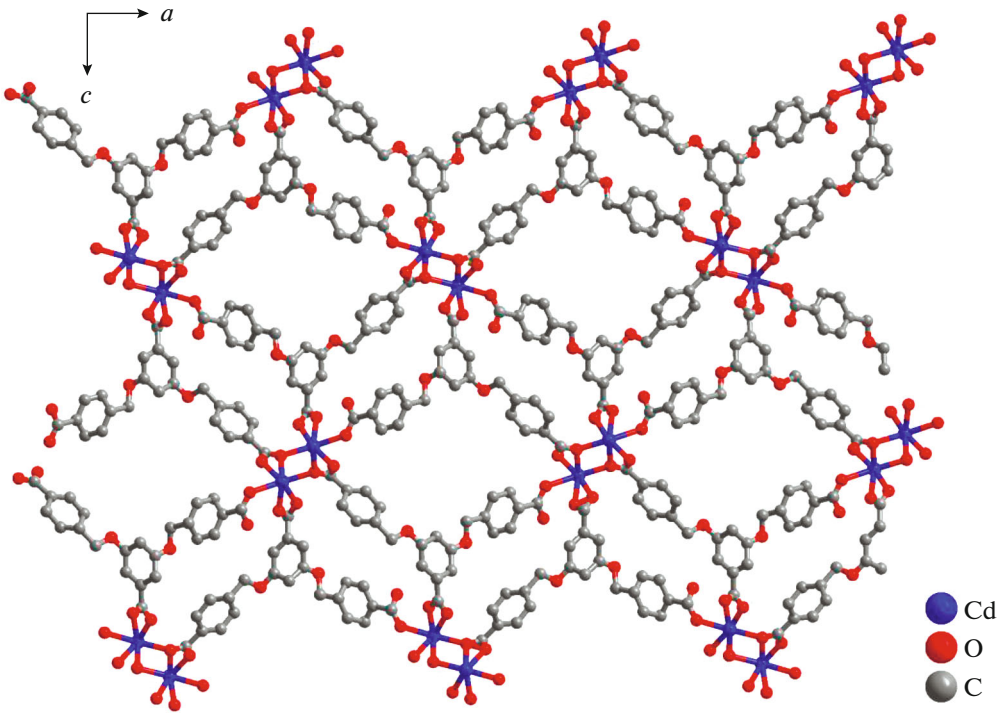

Fig. 4. The 2D pore layer in the *ac* plane of coordination polymer **II**.

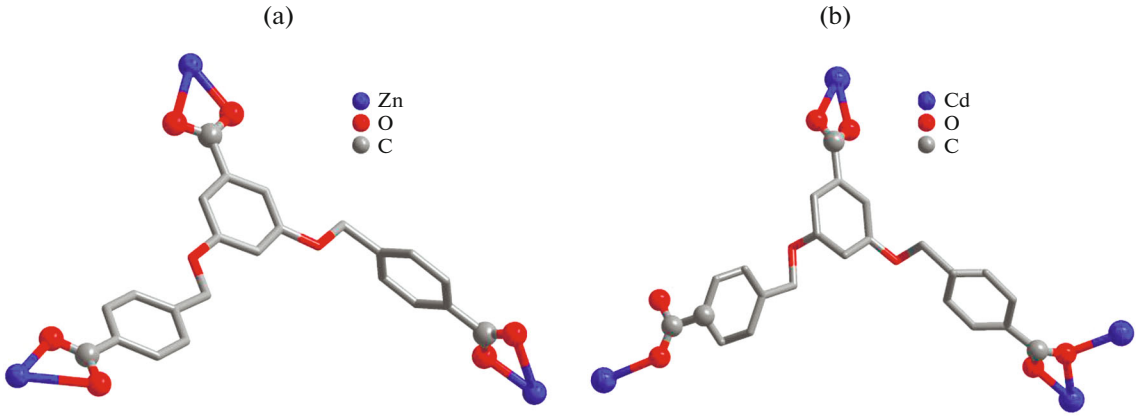

Fig. 5. The different coordination modes of **I** (a), **II** (b).

coordinated Py between 77 and 379°C with a weight loss of 27.86% (calcd. 30.71%). Then at about 379°C, the main framework starts to collapse and the mass losses correspond to the loss of the organic ligands. Complex **I** indicates a weight loss of 53.89% in the range of 379–513°C, which consists of the release of two coordinated $bcpmba^{3-}$ molecule per formula unit (calcd. 54.22%). The remaining weight of 15.71% is in accordance with the mass of ZnO residue (calcd. 15.80%). For **II**, it lost one coordinated water from 30 to 308°C with a weight loss of 3.26% (calcd. 3.29%), and the major framework is stable up to 308°C and then begins to collapse. For complex **II**, a significant weight loss of 72.46% has been observed in the temperature range 308–576°C, corresponding to the consecutive loss of $Hbcpmba^{2-}$ ligands (calcd. 76.68%). The remaining weight of 24.28% is in accordance with the mass of CdO residue (calcd. 23.44%).

Luminescent properties of compounds with d^{10} metal centers have fascinated much attention because of their potential applications in chemical sensors, electroluminescent display, and photochemistry [24]. The solid-state luminescent properties of compounds **I**, **II** as well as free $H_3bcpmba$ ligand were investigated at room temperature under the same experimental conditions and their emission spectra are given (Fig. 7). When excited with 310 nm light, free $H_3bcpmba$ ligand exhibit luminescent spectra with an emission maximum at 419 nm, which can be ascribed to the ligand centered electronic transitions, that is, the $\pi^* \rightarrow n$ or $\pi^* \rightarrow \pi$ transition in nature according to the reported literature [25]. Under the same excitation conditions, compounds **I** and **II** display intense emission peak at 375 and 350 nm, respectively. These emissions are neither metal-to-ligand charge transfer (MLCT) nor ligand-to-metal transfer (LMCT) in nature, since Zn(II) and Cd(II) ions are difficult to

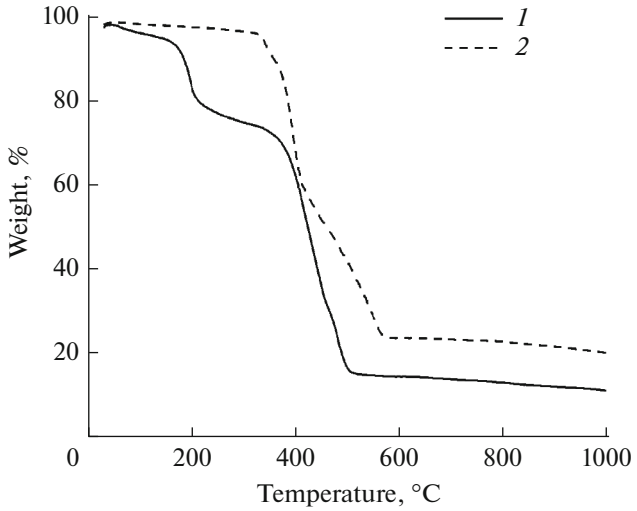

Fig. 6. TG analyses curves of coordination polymer **I** and **II**.

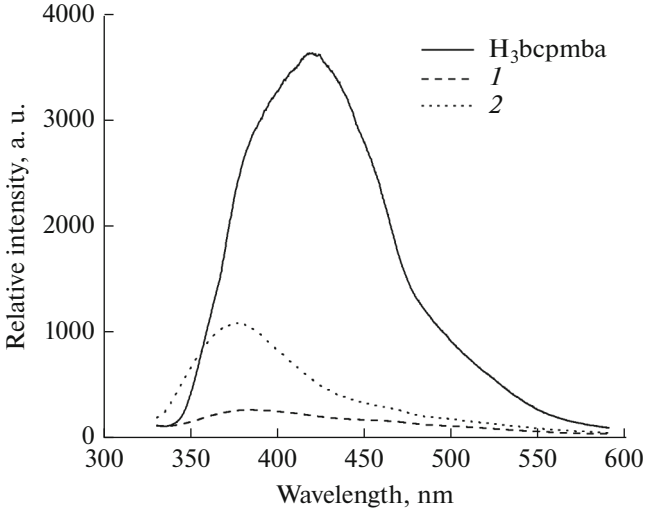

Fig. 7. Fluorescence spectra of $H_3bcpmba$ and complexes **I** and **II** in the solid state at room temperature.

oxidize or reduce due to their d^{10} configuration. They can probably be attributed to the intraligand fluorescent emission [26]. In comparison to that of the free H_3bcpmba, the emission maxima of complexes **I** and **II** are significantly shifted (Fig. 7). The shifts of the emission bands are attributed to the deprotonated effect of a tricarboxylic acid when it is coordinated to Zn(II) and Cd(II) ions [27]. More detailed theoretical and spectroscopic studies may be necessary for a better understanding of the luminescent mechanism.

CONCLUSIONS

In conclusion, we have successfully synthesized and characterized two new coordination polymers based on the semirigid aromatic multicarboxylate ligands by utilizing various metal salts. Complexes **I** and **II** exhibits different 2D porous layered architecture. The results demonstrate that the semirigid aromatic multicarboxylate ligands may be used as a versatile building block to construct novel coordination polymers with fascinating structures and properties. We conclude that the main ligand and the auxiliary ligand have a certain influence on the structure of the complex. In addition, the photoluminescence properties of complexes **I** and **II** were studied in the solid state at room temperature and all compounds possess high thermal stability. This approach may be useful for construction of a variety of new transition metal complexes and luminescent coordination polymers that have potential for new fluorescent materials.

FUNDING

This work is supported by the start-up foundation of Sichuan University of Science and Engineering (no. 2015RC29).

CONFLICT OF INTEREST

The authors declare that they have no conflicts of interest.

SUPPLEMENTARY INFORMATION

The online version contains supplementary material available at https://doi.org/10.1134/S1070328422010067.

REFERENCES

1. Gu, J.Z., Wan, S.M., Kirillova, M.V., and Kirillov, A.M., *Dalton Trans.*, 2020, vol. 49, p. 71971.
2. Ban, Y., Zhao, M., and Yang, W., *Front. Chem. Sci. Eng.*, 2020, vol. 14, p. 188.
3. Tăbăcaru, A., Pettinari, C., and Galli, S., *Coord. Chem. Rev.*, 2018, vol. 372, p. 1.
4. Fan, L.M., Liu, Z.J., Zhang, Y.J., et al., *Inorg. Chem. Commun.*, 2019, vol. 107, p. 107463.
5. Fan, L., Gao, L., Ren, G., et al., *J. Solid State Chem.*, 2018, vol. 264, p. 15.
6. Wang, X.Z., Zhu, D.R., Xu, Y., et al., *Cryst. Growth Des.*, 2010, vol. 10, p. 887.
7. Paz, F.A., Klinowski, J., Vilela, S.M., et al., *Chem. Soc. Rev.*, 2012, vol. 41, p. 945.
8. Gu, J.Z., Cui, Y.H., Liang, X.X., et al., *Cryst. Growth Des.*, 2016, vol. 16, p. 4658.
9. Shao, Y.L., Cui, Y.H., Gu, J.Z., et al., *RSC Adv.*, 2015, vol. 5, p. 87484.
10. Wu, W.P., Liu, P., Liang, Y.T., et al., *J. Solid State Chem.*, 2015, vol. 228, p. 124.
11. Wang, L., Yang, G.P., Yan, Y.T., et al., *RSC Adv.*, 2017, vol. 7, p. 46125.
12. Mu, Y.J., Fu, J.H., Song, Y.J., et al., *Cryst. Growth Des.*, 2011, vol. 11, p. 2183.
13. Du, M., Li, C.P., Liu, C.S., and Fang, S.M., *Coord. Chem. Rev.*, 2013, vol. 257, p. 1282.
14. Xia, C.K., Wu, F., Yang, K., et al., *Polyhedron*, 2016, vol. 117, p. 637.
15. SAINT, Version 6.02a, Madison: Bruker AXS Inc., 2002.
16. Krause, L., Herbst-Irmer, R., Sheldrick, G.M., and Stalke, D., *J. Appl. Cryst.*, 2015, vol. 48, p. 3.
17. Sheldrick, G.M., *SHELXS 97, Program for Crystal Structure Solution*, Göttingen: Univ. of Göttingen, 1997.
18. Sheldrick, G.M., *SHELXL 97, Program for Crystal Structure Refinement*, Göttingen: Univ. of Göttingen, 1997.
19. Sluis, P.V.D. and Spek, A.L., *Acta Crystallogr., Sect, A: Found. Crystallogr.*, 1990, vol. 46, p. 194.
20. Zhang, S., He, H., Sun, F., et al., *Inorg. Chem. Commun.*, 2017, vol. 79, p. 55.
21. Zhou, L., Zhao, K., Dong, H.Y., et al., *Inorg. Chem. Commun.*, 2017, vol. 79, p. 17.
22. Wang, L., Yang, G.P., Yan, Y.T., et al., *RSC Adv.*, 2017, vol. 7, p. 46125.
23. Cui, J.H., Yang, Q.X., Li, Y.Z., et al., *Cryst. Growth Des.*, 2013, vol. 13, p. 1694.
24. Huang, Q., Huang, J.H., Gu, L., et al., *RSC Adv.*, 2018, vol. 8, p. 557.
25. Xie, S.L., Wang, H.F., Liu, ZH., et al., *RSC Adv.*, 2015, vol. 5, p. 7121.
26. Miao, S.B., Li, Z.H., Xu, C.Y., and Ji, B.M., *CrystEngComm*, 2016, vol. 18, p. 4636.
27. Ma, L.F., Qin, J.H., Wang, L.Y., and Li, D.S., *RSC Adv.*, 2011, vol. 1, p. 180.